# Symmetry-protected single-photon subradiance

Han Cai, Da-Wei Wang, Anatoly A. Svidzinsky, Shi-Yao Zhu, and Marlan O. Scully

# Symmetry protected single photon subradiance

Han Cai[1], Da-Wei Wang[1], Anatoly A. Svidzinsky[1], Shi-Yao Zhu[2] and Marlan O. Scully[1,3,4]

[1] Texas A&M University, College Station TX 77843; [2] Beijing Computational Science Research Center, Beijing, China; [3] Princeton University, Princeton NJ 08544; [4] Baylor University, Waco, TX 76706

We study the protection of subradiant states by the symmetry of the atomic distributions in the Dicke limit, in which collective Lamb shifts cannot be neglected. We find that anti-symmetric states are subradiant states for distributions with reflection symmetry. Continuous symmetry can also be used to achieve subradiance. This study is relevant to the problem of robust quantum memory with long storage time and fast readout.

Cooperative spontaneous emission (Dicke superradiance [1]) and the cooperative vacuum induced levels shifts (Lamb shifts [2]) are hot topics in quantum optics. For extended ensembles when the size of the atomic cloud is much larger than the wavelength, the directional emission [3, 4] and collective Lamb shift [5] of single photon superradiance [3, 6–13] have attracted much interest. Recently it has been shown [14] that it is possible to use subradiance (the cooperative suppression of spontaneous emission [13]) to store a photon in a small volume for many atomic lifetimes; and later switch the subradiant state to a superradiant state which emits a photon in a small fraction of an atomic lifetime. Such a process has potential applications in e.g., quantum informatics.

It has been proved that the distribution of the atoms (e.g., periodic or random) in an extended ensemble has a substantial effect on cooperative spontaneous emission [15]. However, the effect of the atomic distribution in the Dicke limit has been studied only a little. Since the distance between atoms is much smaller than the wavelength, one might guess that the distribution of atoms is not important. We here show that the collective Lamb shift cannot be neglected in general. However, by analyzing the relation between the symmetry of the atomic distribution and cooperative emission, we demonstrate the mitigation of the collective Lamb shift and the symmetry protected subradiance.

The $N$-atom sample (size much smaller compared to the transition wavelength $\lambda$) excited by a single photon can be described by the Dicke state

$$|+\rangle = \frac{1}{\sqrt{N}} \sum_{j=1}^{N} |j\rangle, \tag{1}$$

where $|j\rangle = |b_1, b_2...a_j...b_N\rangle$, $a_j(b_j)$ is the excited (ground) state of the $j$th atom. Since the size of atom is much smaller than the wavelength of the coupling field, we could use dipole approximation. It also allows us to distribute many atoms within one wavelength, which is called the Dicke limit. The probability amplitude of the state (1) decays at the rate $\Gamma_+ = N\gamma$ where $2\gamma$ is the single atom population decay rate. In the "opposite" case, if we neglect Lamb shift, the single photon subradiance

state

$$|-\rangle = \frac{1}{\sqrt{N}} (\sum_{j=1}^{N/2} |j\rangle - \sum_{j=N/2+1}^{N} |j\rangle), \tag{2}$$

does not decay, i.e., $\Gamma_- = 0$ because of the destructive interference of the atomic transitions. However, when the cooperative Lamb shifts, i.e., the effects of emission and reabsorption of virtual photons, are counted in, it can degrade superradiance [5, 16, 17]. In single photon superradiance, this does not overwhelm the collective enhancement of spontaneous emission. Not so in the case of subradiance, the collective Lamb shift can now destroy the ability of the atoms to "store" light, i.e., the original subradiant states are not necessarily subradiant anymore. For random atomic distribution, since each atom "sees" different neighboring atoms, collective Lamb shift type fluctuation induced dephasing significantly degrades the destructive interference.

We first turn to a more detailed study of the lifetime of the $|-\rangle$ state and the way in which collective Lamb shift type fluctuations influence the state evolution. Numerically calculated population decay of the anti-symmetric $|-\rangle$ state with and without taking into account virtual transitions is compared in Fig.1. The Dicke limit ensemble of 100 atoms are randomly distributed along a 1D line within $0.01\lambda$, where $\lambda$ is the atomic transition wavelength. Fig.1 shows that collective Lamb shifts $\Omega_{ij}$ degrade subradiance of the state $|-\rangle$. Without Lamb shifts, $|-\rangle$ is subradiant. Counting in the Lamb shifts, $|-\rangle$ is composed by both superradiant and subradiant eigenstates. The components of the superradiant eigenstate decay fast, leaving slowly decaying subradiant components.

The simulation is performed in the basis of single-photon eigenstate. The eigenstates decay exponentially, i.e., $|\psi_n(t)\rangle = \sum_j \beta_j e^{-\Lambda_n t/\hbar} |j\rangle$, with $\Lambda_n$ being the $n$th complex eigenvalue and $\beta_j$ being the probability amplitude to find atom $j$ excited. The eigenvalue equations are[11, 18]

$$\Lambda_n \beta_i = \gamma \beta_i - i \sum_{i \neq j}^{N} (-\Omega_{ij} + i\gamma_{ij})\beta_j = \sum_j^N M_{ij}\beta_j, \tag{3}$$

where $\Omega_{ij} = -\frac{\cos(k_0 r_{ij})}{k_0 r_{ij}}\gamma$, with $k_0$ the transition wave vector and $r_{ij}$ the distance between atoms $i$ and $j$, is the
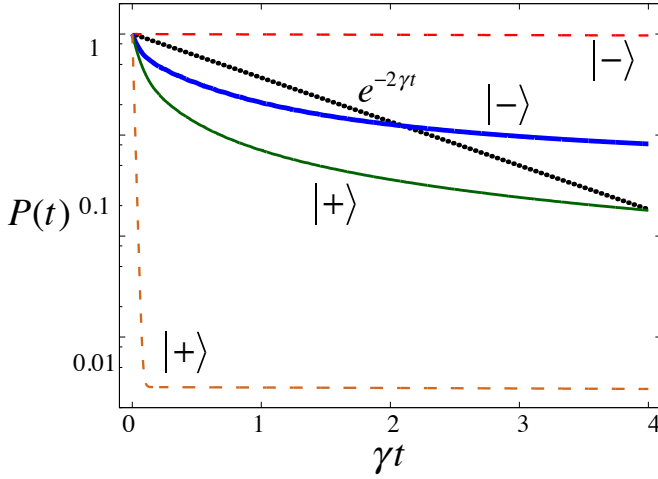
Figure 1. Probability $P(t) = \langle\Psi(t)|\Psi(t)\rangle$ to find atoms excited as a function of time for atoms initially prepared in the $|+\rangle$ and $|-\rangle$ states. The solid curve takes the cooperative Lamb shift into consideration, causing rapid decay for both $|+\rangle$ and $|-\rangle$. The dashed curve ignores the Lamb shift. For comparison, we also plot single-atom decay curve $e^{-2\gamma t}$ (dot line).
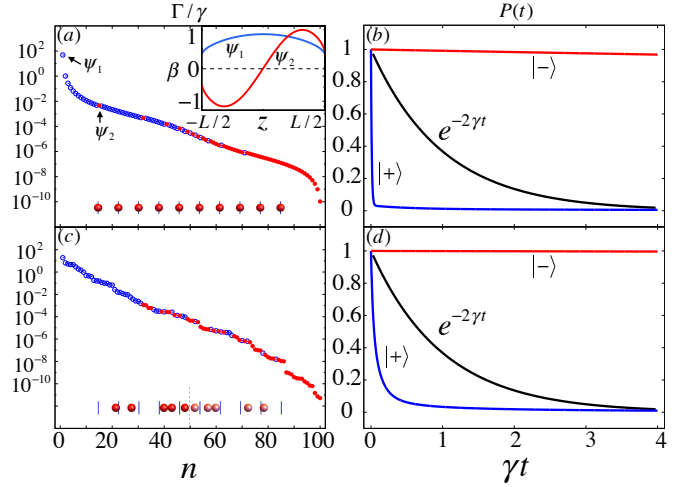


Figure 2. (a) Distribution of decay rates for eigenstates of an ensemble of 100 atoms regularly placed along a line with spacing between adjacent atoms $0.0001\lambda$. Blue empty dots are symmetric states while red solid dots are anti-symmetric states. Inset: Probability amplitude $\beta_j$ as a function of the coordinate of the $j$th atom $z_j$ for the fastest decaying symmetric (blue line) and anti-symmetric (red line) states. (b) Population decay of states $|+\rangle$ and $|-\rangle$ as a function of time. Single-atom exponentially decaying curve is shown for comparison. (c) and (d): The same as in (a) and (b), but for random spatial distribution of atoms with reflection symmetry.

collective Lamb shift, $\gamma_{ij} = \frac{\sin(k_0 r_{ij})}{k_0 r_{ij}}\gamma$ is the collective decay rate, and $M_{ij} = \gamma\delta_{ij} + (i\Omega_{ij} + \gamma_{ij})(1-\delta_{ij})$ with $\delta_{ij}$ the Kronecker delta function are the elements of the evolution matrix $\mathbf{M}$. This result is based on a scalar radiation field, which can be regarded as the average effect of the vector field [19, 20]. We use scalar field throughout this paper for simplicity. Results for vector field are shown in Appendix A. There is no essential difference between the results of scalar and vector field. Numerically calculating all eigenvalues $\Lambda_n$ by diagonalization of the matrix $\mathbf{M}$, we obtain $|\Psi(t)\rangle = \sum_n c_n e^{-\Lambda_n t}|\psi_n\rangle$, here $c_n = \langle\psi_n^T|\Psi(0)\rangle$ is the projection of initial state to the single-photon Dicke-Lamb eigenstate, and $\langle\psi_n^T|$ is the transpose of $|\psi_n\rangle$ (since the matrix $\mathbf{M}$ is symmetric instead of Hermitian).

The mitigation of the collective Lamb shifts by arranging the atom distribution in a ring has been found useful in maintaining superradiance [21]. If the atoms are distributed randomly, the transition frequencies of atoms are different due to the different environment of each atom, superradiance is destroyed. However, if they are arranged periodically on a ring, all atoms have the same environment and the superradiance is recovered. It sheds light on the importance of the symmetry of the atomic distribution.

Symmetry has long been investigated as a central feature of superradiance [4]. In Dicke's original paper [1], it was noted that the most decaying excited state of the collective atomic distribution must be symmetric since the ground state is symmetric and the Hamiltonian preserves symmetry. The symmetry of the atomic distribution determines the symmetry of the eigenstates. For the sake of simplicity, we take 1D atomic distribution preserving reflection symmetry for example. We set $z$

along the line of atoms and $z = 0$ as the middle point of the atomic ensemble. The mirror reflection operator $\pi$, which transforms $z \to -z$, commutes with the matrix $\mathbf{M}$ for a periodic distribution of atoms, $[\mathbf{M}, \pi] = 0$. A non-degenerate eigenstate of $\mathbf{M}$ is also an eigenstate of $\pi$ [22]. $N$ eigenstates of $N$ atoms excited by a single photon are separated into two groups with opposite eigenvalues of $\pi$, i.e., $N/2$ symmetric and $N/2$ anti-symmetric states.

In the Dicke limit, the ensemble size is much smaller than the transition wavelength. If we neglect the collective Lamb shifts $\Omega_{ij}$ in Eq.(3), we obtain $M_{ij} = \gamma$ for all $i$ and $j$. In this case the eigenvalues of $\mathbf{M}$ are $\Lambda_1 = N\gamma$ and all others are equal to zero, i.e., there is one superradiant state and $N-1$ subradiant states [20]. The superradiant eigenstate is the symmetric state $|+\rangle$. Any state orthogonal to this state is subradiant, for example, the anti-symmetric state $|-\rangle$. With the presence of $\Omega_{ij}$, $|-\rangle$ is not subradiant any more, as shown in Fig.1.

We can recover the subradiant nature of $|-\rangle$ state by rearranging atoms such that their distribution possesses reflection symmetry, i.e., $z_j = -z_{N+1-j}$ and $\pi^\dagger \mathbf{M}\pi = \mathbf{M}$. In Fig.2(b) we plot the population decay for periodic distribution of atoms. The decay of $|+\rangle$ is enhanced compared with the case of random distribution, which is consistent with Ref. [21]. On the other hand, the decay of $|-\rangle$ state is drastically inhibited.

To analyze the reason of this inhibition, we plot $\beta_j$ for the superradiant state $|\psi_1\rangle$ and for a subradiant state

$|\psi_2\rangle$ in the inset of Fig.2(a). It is clear that the state $|\psi_1\rangle$ is symmetric with respect to the center of the sample. There is only one superradiant state $|\psi_1\rangle$ with decay rate $\sim N\gamma$, as shown in Fig.2(a). The anti-symmetric state $|-\rangle$ is orthogonal to the superradiant state $|\psi_1\rangle$. Because of the Dicke limit, the superradiant state $|\psi_1\rangle$ shown in the inset of Fig.2(a) is similar to a uniform probability amplitude state $|+\rangle$.

Since reflection symmetry is the key point in the above analysis, it is not necessary for atoms to be periodically distributed to make the $|-\rangle$ state subradiant. In Fig.2(c), we allow half of the atoms to be distributed randomly, but in reflection symmetry with the other half. The population decay of $|-\rangle$ state is still substantially inhibited as shown in Fig.2(d). This is because the superradiant state $|\psi_1\rangle$ for random atomic distribution is still symmetric and has no overlap with the $|-\rangle$ state.

Generally, in the Dicke limit, we have one superradiant and $N-1$ subradiant eigenstates. Atomic distribution determines the symmetry of the superradiant state. By preparing atoms in an orthogonal state to this superradiant eigenstate, we can reach subradiance and store the photon. To release the photon, we can coherently change the state to have the same symmetry as the superradiant eigenstate and achieve a rapid readout [14].

We could achieve subradiance in extended sample as well. For an extended spherical sample, we find [14] approximately decay rates $\Gamma_+^{\vec{k}_0} \cong \gamma[1 + \frac{3}{8\pi}\frac{\lambda^2}{A}(N-1)]$ and $\Gamma_-^{\vec{k}_0} \cong \gamma[1 - \frac{3}{8\pi}\frac{\lambda^2}{A}]$ for states $|\pm\rangle_{\vec{k}_0} = \sum_{j=1}^{N/2} e^{i\vec{k}_0 \cdot \vec{r}_j}|j\rangle \pm \sum_{j=N/2+1}^{N} e^{i\vec{k}_0 \cdot \vec{r}_j}|j\rangle$, where $\lambda$ is the transition wavelength, $R$ is the radius of the atomic cloud and $A = \pi R^2$ is the cross section area. The "extra" $\gamma$ in $\Gamma_+^{\vec{k}_0}$ is not important, as it is small compared to the leading term going as $\frac{3}{8\pi}\frac{\lambda^2}{A}N$. However the $\gamma$ term in $\Gamma_-^{\vec{k}_0}$ is important. It seems like for the $|-\rangle_{\vec{k}_0}$ state, the single atom spontaneous decay rate is a lower decay limit for an extended sample. The good news however is that the collective spontaneous decay can also be mitigated by the spatial symmetry of the atomic distribution. In order to calculate the the evolution of atomic system of a dense cloud of volume $V$, we use equation with exponential kernel [10]

$$\frac{\partial \beta(t, \mathbf{r})}{\partial t} = i\gamma \int d\mathbf{r}' n(\mathbf{r}') \frac{\exp(ik_0|\mathbf{r}-\mathbf{r}'|)}{k_0|\mathbf{r}-\mathbf{r}'|}\beta(t, \mathbf{r}'), \quad (4)$$

where $\beta(t, \mathbf{r})$ is the probability amplitude to find atom at position $\mathbf{r}$ excited at time $t$, $n(\mathbf{r})$ is the atomic density. Eq.(4) is valid in Markovian (local) approximation and is the continuous limit of Eq.(3). Eigenfunctions of Eq.(4) are $\beta(t, \mathbf{r}) = e^{-\Lambda t}\beta(\mathbf{r})$ and the eigenvalues $\Lambda$ determine the evolution of the atomic system. $\mathrm{Re}(\Lambda)$ yields the state decay rate, while $\mathrm{Im}(\Lambda)$ describes frequency (Lamb) shift of the collective excitation. The eigenfunction equation for $\beta(\mathbf{r})$ reads

$$-i\gamma \int d\mathbf{r}' n(\mathbf{r}') \frac{\exp(ik_0|\mathbf{r}-\mathbf{r}'|)}{k_0|\mathbf{r}-\mathbf{r}'|}\beta(\mathbf{r}') = \Lambda \beta(\mathbf{r}). \quad (5)$$

We consider an infinitely long cylindrical shell of radius $R$ and use cylindrical coordinates $\mathbf{r} = (\rho, \varphi, z)$. The atomic density is $n(\mathbf{r}) = n_0 \delta(\rho - R)/2\pi R$, where $n_0$ is the number of atoms per unit length of the cylinder. For such geometry Eq.(5) reads

$$-\frac{i\gamma n_0}{2\pi} \int_0^{2\pi} d\varphi' \int_{-\infty}^{\infty} dz' K(\varphi-\varphi', z-z')\beta(\varphi', z') = \Lambda\beta(\varphi, z), \quad (6)$$

where

$$K(\varphi, z) = \frac{\exp[ik_0\sqrt{2R^2 - 2R^2\cos\varphi + z^2}]}{k_0\sqrt{2R^2 - 2R^2\cos\varphi + z^2}}.$$

We look for solution of Eq.(6) in the form

$$\beta(\varphi, z) = e^{in\varphi} e^{ik_z z}, \quad (7)$$

where $n$ is an integer number and $k_z$ is the wave number of the mode along the cylindrical axis $z$. Substituting Eq.(7) in Eq.(6) we obtain the following equation for eigenvalues $\Lambda_n$

$$\Lambda_n = -\frac{i\gamma n_0}{2\pi} \int_0^{2\pi} d\varphi' \int_{-\infty}^{\infty} dz' K(\varphi', z')e^{in\varphi'} e^{ik_z z'}. \quad (8)$$

Integrating over $z'$ can be done by using the integral

$$\int_{-\infty}^{\infty} dz' \frac{exp[ik_0\sqrt{r^2 + z'^2}]}{\sqrt{r^2 + z'^2}}e^{ik_z z'} = i\pi H_0^{(1)}(r\sqrt{k_0^2 - k_z^2}), \quad (9)$$

where $H_0^{(1)}(x)$ is the Hankel function. Then Eq.(8) reduces to

$$\Lambda_n = \frac{\gamma n_0}{2k_0} \int_0^{2\pi} d\varphi' H_0^{(1)}(R\sqrt{2-2\cos\varphi'}\sqrt{k_0^2 - k_z^2})e^{in\varphi'}. \quad (10)$$

The integration over $\varphi'$ can be calculated using

$$\int_0^{2\pi} d\varphi' H_0^{(1)}(a\sqrt{2-2\cos\varphi'})e^{in\varphi'} = 2\pi J_n(a)H_n^{(1)}(a), \quad (11)$$

and Eq.(10) leads to

$$\Lambda_n = \frac{\pi\gamma n_0}{k_0} J_n(R\sqrt{k_0^2 - k_z^2})H_n^{(1)}(R\sqrt{k_0^2 - k_z^2}). \quad (12)$$

Hankel functions can be written as a combination of the Bessel functions of the first and the second kind as

$$H_n^{(1)}(x) = J_n(x) + iY_n(x), \quad (13)$$

which yields the following answer for the real and imaginary parts of the eigenvalues $\Lambda_n$ for $k_z \leq k_0$

$$\Gamma_n = \mathrm{Re}(\Lambda_n) = \frac{\pi\gamma n_0}{k_0} J_n^2(R\sqrt{k_0^2 - k_z^2}), \quad (14)$$
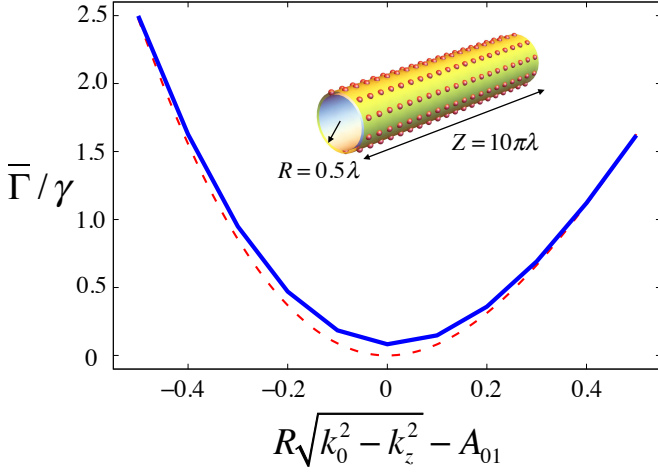
Figure 3. Solid line shows the average decay rate $\bar{\Gamma}$ of $\beta_{0,k_z}$ state for periodic distribution of atoms on cylindrical surface sketched on the top. The cylinder consists of 1000 atoms in 100 layers with 10 atoms per each layer. Radius of the cylinder is $R = 0.5\lambda$ and the distance between adjacent layers is $0.1\pi\lambda$. Analytical result (14) for an infinitely long cylindrical shell with $100/\pi\lambda$ atoms per unit length is plotted as dashed line. The horizontal axis is deviation of the $R\sqrt{k_0^2 - k_z^2}$ from the root $A_{01}$ of the Bessel function $J_0(x)$. $\bar{\Gamma} = -\gamma \ln[P(1/\gamma)]$ is defined as average decay rate for time scale of $1/\gamma$.

$$\Delta_n = \text{Im}(\Lambda_n) = \frac{\pi\gamma n_0}{k_0} J_n(R\sqrt{k_0^2 - k_z^2}) Y_n(R\sqrt{k_0^2 - k_z^2}).$$
$$(15)$$

Eq.(14) shows that timed-Dicke state ($n = 0$ and $k_z = k_0$) $\beta(\varphi, z) = e^{ik_0 z}$ has the fastest decay rate $\text{Re}(\Lambda_{\text{TD}}) = \pi\gamma n_0/k_0$. However, collective Lamb shift for such state logarithmically diverges since $Y_0(x) \approx (2/\pi)\ln(x/2)$ for small $x$. For the states with $R\sqrt{k_0^2 - k_z^2} = A_{nl}$ where $A_{nl}$ is $l$th zero of the Bessel function $J_n(x)$, such as the state $\beta_{n,k_z}(\varphi, z) = e^{in\varphi} e^{iz\sqrt{k_0^2 - A_{nl}^2/R^2}} \approx e^{i(k_0 - A_{nl}^2/2k_0 R^2)z} e^{in\varphi}$, the decay rate and the collective Lamb shift vanish. In Fig.3, we compare the decay of axially symmetric atomic states for continuous and discrete distribution of atoms on cylindrical surface. Namely, we plot the average decay rate $\bar{\Gamma} = -\gamma \ln P(1/\gamma)$ of the state $\beta_{0,k_z}(\phi, z) = e^{ik_z z}$, where $P(t)$ is the probability to find atoms excited, as a function of $R\sqrt{k_0^2 - k_z^2} - A_{01}$, where $A_{01} = 2.404$ is the first zero of $J_0(x)$. The average decay rate approaches zero when $R\sqrt{k_0^2 - k_z^2} = A_{01}$ for a discrete periodic atomic distribution shown in Fig.3. This agrees with the analytical result in the continuous limit in Eq.(14) plotted as a dashed line. Cylindrical atomic distribution can be achieved, e.g., by adhering nano diamond with NV centers or SiV centers on a carbon tube.

In summary, we demonstrate that the collective Lamb shifts that are usually thought to destroy subradiance can be mitigated by symmetry. For atomic distributions with mirror symmetry (a discrete symmetry), the anti-symmetry states are subradiant, even when half of the atoms are randomly distributed as long as the mirror
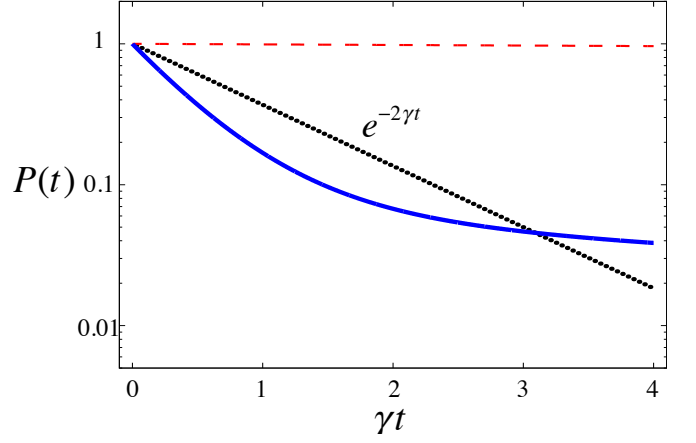


Figure 4. Results for vector field with $\Omega_{ij}^v$ and $\gamma_{ij}^v$. The atomic distribution is the same as Fig.1 in main text. Probability $P(t)$ to find atoms excited as a function of time for atoms initially prepared in the $|-\rangle$ state. The solid curve takes the cooperative Lamb shift into consideration. The dashed curve ignores the Lamb shift. For comparison, we also plot single-atom decay curve $e^{-2\gamma t}$ (dot line).

symmetry is maintained. Periodic distribution with intrinsic mirror symmetry can be realized in ion traps and the subradiant anti-symmetry states can be prepared by specially tailored anti-symmetric optical modes. In addition, continuous symmetry can also be used to realize subradiance.

## Appendix A: Results with vector field

For the sake of simplicity, we use scalar field theory throughout the main text, i.e.,

$$\Omega_{ij} = -\frac{\cos(k_0 r_{ij})}{k_0 r_{ij}}\gamma, \qquad (A1)$$

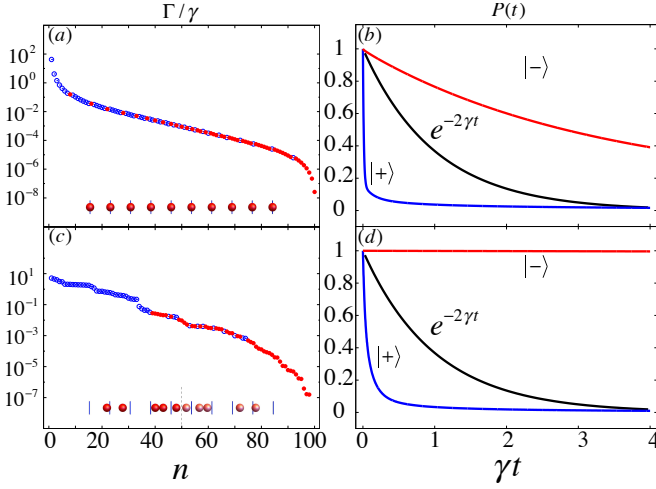$$\gamma_{ij} = \frac{\sin(k_0 r_{ij})}{k_0 r_{ij}}\gamma. \qquad (A2)$$

Figure 5. Eigenvalue distribution and population evolution for vector field. (a) Distribution of decay rates for eigenstates of an ensemble of 100 atoms regularly placed along a line with spacing between adjacent atoms $0.0006\lambda$. Blue empty dots are symmetric states while red solid dots are anti-symmetric states. (b) Population decay of states $|+\rangle$ and $|-\rangle$. Single-atom exponentially decaying curve is shown for comparison. (c) and (d): The same as in (a) and (b), but for random distribution of atoms with reflection symmetry.

However, if the polarization of electromagnetic field is considered, $\Omega_{ij}$ and $\gamma_{ij}$ are[21]

$$\Omega_{ij}^v = \frac{3}{4}\gamma[-P_{ij}\frac{\cos kr_{ij}}{kr_{ij}} + Q_{ij}(\frac{\sin kr_{ij}}{(kr_{ij})^2} + \frac{\cos kr_{ij}}{(kr_{ij})^3})] \quad (A3)$$

$$\Gamma_{ij}^v = \frac{3}{4}\gamma[P_{ij}\frac{\sin kr_{ij}}{kr_{ij}} + Q_{ij}(\frac{\cos kr_{ij}}{(kr_{ij})^2} - \frac{\sin kr_{ij}}{(kr_{ij})^3})], \quad (A4)$$

where factors $P_{ij} = \hat{\mu}_i \cdot \hat{\mu}_j - (\hat{\mu}_i \cdot \hat{r}_{ij})(\hat{\mu}_j \cdot \hat{r}_{ij})$ and $Q_{ij} = \hat{\mu}_i \cdot \hat{\mu}_j - 3(\hat{\mu}_i \cdot \hat{r}_{ij})(\hat{\mu}_j \cdot \hat{r}_{ij})$, $\hat{r}_{ij} = \hat{r}_i - \hat{r}_j$. Here $\hat{r}_j$ and $\hat{\mu}_j$ are the position and dipole of the $j$th atom respectively. In Fig.4, the features of the curve is the same as in Fig.1. Collective Lamb shift $\Omega_{ij}^v$ significantly degrades the subradiance of the state $|-\rangle$. In Fig.5, we could restore subradiance by taking advantage of the symmetry of atomic distribution, which is similar to the result of Fig.2 with scalar field.

[1] R. Dicke, Phys. Rev. **93**, 99110 (1954).
[2] W. E. Lamb Jr and R. C. Retherford, Phys. Rev. **72**, 241 (1947).
[3] M. O. Scully, E. S. Fry, C. H. R. Ooi, and K. Wódkiewicz, Phys. Rev. Lett. **96**, 010501 (2006).
[4] A. Crubellier, S. Liberman, and P. Pillet, Opt. Comm. **33**, 143 (1980).
[5] R. Röhlsberger, Fortschritte der Physik **61**, 360 (2013).
[6] C. H. van der Wal, M. D. Eisaman, A. André, R. L. Walsworth, D. F. Phillips, A. S. Zibrov, and M. D. Lukin, Science (New York, N.Y.) **301**, 196 (2003).
[7] A. T. Black, J. K. Thompson, and V. Vuletić, Phys. Rev. Lett. **95**, 133601 (2005).
[8] A. Kuzmich, W. P. Bowen, A. D. Boozer, A. Boca, C. W. Chou, L. M. Duan, and H. J. Kimble, Nature **423**, 731 (2003).
[9] V. Balic, D. A. Braje, P. Kolchin, G. Y. Yin, and S. E. Harris, Phys. Rev. Lett. **94**, 183601 (2005).
[10] A. Svidzinsky and J.-T. Chang, Phys. Rev. A **77**, 043833 (2008).
[11] A. A. Svidzinsky, J.-T. Chang, and M. O. Scully, Phys. Rev. A **81**, 053821 (2010).
[12] D.-W. Wang, R.-B. Liu, S.-Y. Zhu, and M. O. Scully, Phys. Rev. Lett. **114**, 043602 (2015).
[13] A. A. Svidzinsky, X. Zhang, and M. O. Scully, Phys. Rev. A **92**, 013801 (2015).
[14] M. O. Scully, Phys. Rev. Lett. **115**, 243602 (2015).
[15] W. Feng, Y. Li, and S.-Y. Zhu, Phys. Rev. A **89**, 013816 (2014).
[16] R. Friedberg, S. R. Hartmann, and J. T. Manassah, Phys. Rep. **7**, 101 (1973).
[17] M. O. Scully and A. A. Svidzinsky, Science **328**, 1239 (2010).
[18] T. Bienaimé, R. Bachelard, N. Piovella, and R. Kaiser, Fortschritte der Physik **61**, 377 (2013).
[19] G. S. Agarwal, *Quantum statistical theories of spontaneous emission and their relation to other approaches* (Springer, 1974).
[20] E. Akkermans, A. Gero, and R. Kaiser, Phys. Rev. Lett. **101**, 103602 (2008).
[21] M. Gross and S. Haroche, Phys. Rep. **93**, 301 (1982).
[22] J. J. Sakurai and J. J. Napolitano, *Modern quantum mechanics* (Pearson Higher Ed, 2014).